Shaken, Not Stirred: Lack of Magma-chamber Overturn in a Caldera Setting Recorded by Whole-pumice, Mineral, and Melt Inclusion Chemistry. The Tshirege Member of the Bandelier Tuff, New Mexico, USA

V15B-0099

Boro, Joseph. R.[1], jboro@hawaii.edu; Wolff, J.A.[2]; Neill, O.K.[3]; Steiner, A.[2]; Shea, T.[1]; Ramos F.C.[4]

Department of Earth Sciences, University of Hawaii, Manoa[1]; School of the Environment, Washington State University[2]; School of Earth and Environmental Sciences, University of Michigan[3]; Department of Geological Sciences, New Mexico State University[4]

1. Introduction and background

Future VEI7+ eruptions pose a significant threat to humanity and understanding the processes which operate to prime one of these systems for eruption is therefore important. The 1.26 Ma eruption of the Tshirege Member of the Bandelier Tuff serves as a natural window into a system which produced once such eruption.

In this study we present data which highlight our efforts to quantify the pre-eruptive thermal conditions of the Tshirege magma chamber and the mechanisms by which the eruption was initiated.

The Valles caldera resulted from two ignimbrite-forming eruptions that produced the Otowi (1.60 ± 0.02 Ma, Wolff and Ramos, 2014) and Tshirege (1.256 ± 0.010 Ma, Phillips et al., 2007) Members of the Bandelier Tuff; the resulting calderas from each eruption are nested. The ~300 – 400 km³ Otowi Member (Cook et al., 2016) consists exclusively of crystal-poor (~5 – 25%), highly evolved high-silica rhyolite with strong zonation in trace elements, and represents melt that separated from a large volume of alkali feldspar + quartz crystalline residue (Wolff and Ramos, 2014; Wolff et al., 2015).

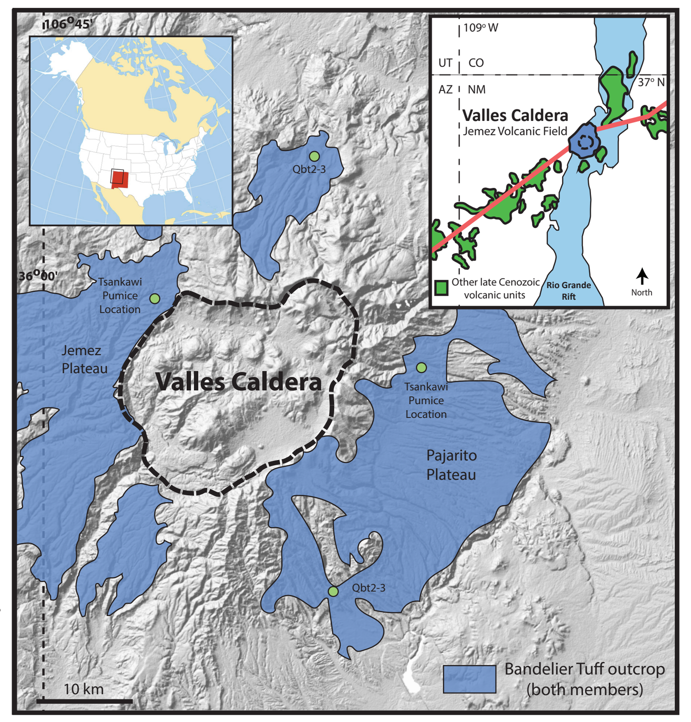

Fig 1. Map showing the location of the Valles Caldera with mapped Bandelier Tuff in blue (Gardner et al., 2010); sample locations for this study labeled with red dots.

2. Tshirege Member Zoning

The ~400 km3 Tshirege Member is also compositionally zoned (Goff et al., 2014; Self et al., 1996; Smith and Bailey, 1966; Wilcock et al., 2013). It consists of a plinian fallout, the Tsankawi Pumice Bed (Qbts), followed by a series of ignimbrite units (Qbt1-5, Figure 2; nomenclature of Warren et al., 2007), and exhibits a broader compositional range than the Otowi Member, from high-silica rhyolite (HSR) to low-silica rhyolite (LSR) with a minor (~1% by volume) dacite component. The LSR pumice is absent from the Tsankawi and lower flow units; it has overall lower concentrations of incompatible elements (e.g. Rb, Nb, Th, U) and higher compatible trace elements (e.g. V, Ba, Sr) compared to the HSR. Upper flow units are more densely welded and thermally altered. Individual fiammé within the welded zones contain crystals which are chemically and morphologically akin to those found in fresh, glassy LSR and HSR pumices. Crystal content of pumice increases upwards from ~10% in the Tsankawi up to ~45% in Qbt4 LSR fiammé; LSR pumice contain characteristic large crystal clots and lenses of sanidine (0.1-2 cm - long axis) plus ortho- and clinopyroxene, with total crystallinities of 25-45%. Some large sanidine clots appear to be aggregate glomerocrsts, while others are partly digested crystals which are optically continuous. Such increases in crystallinity with eruption progress in silicic tuffs have been inferred to imply, by extrapolation, the existence of a non-erupted volume of complementary crystal mush, both specifically for the Bandelier Tuff (Wolff et al., 2015), the similar Bishop Tuff (Hildreth, 2004; Hildreth and Wilson, 2007) and more generally (Bachmann and Bergantz, 2004, 2008).

The Tshirege Member of the Bandelier Tuff

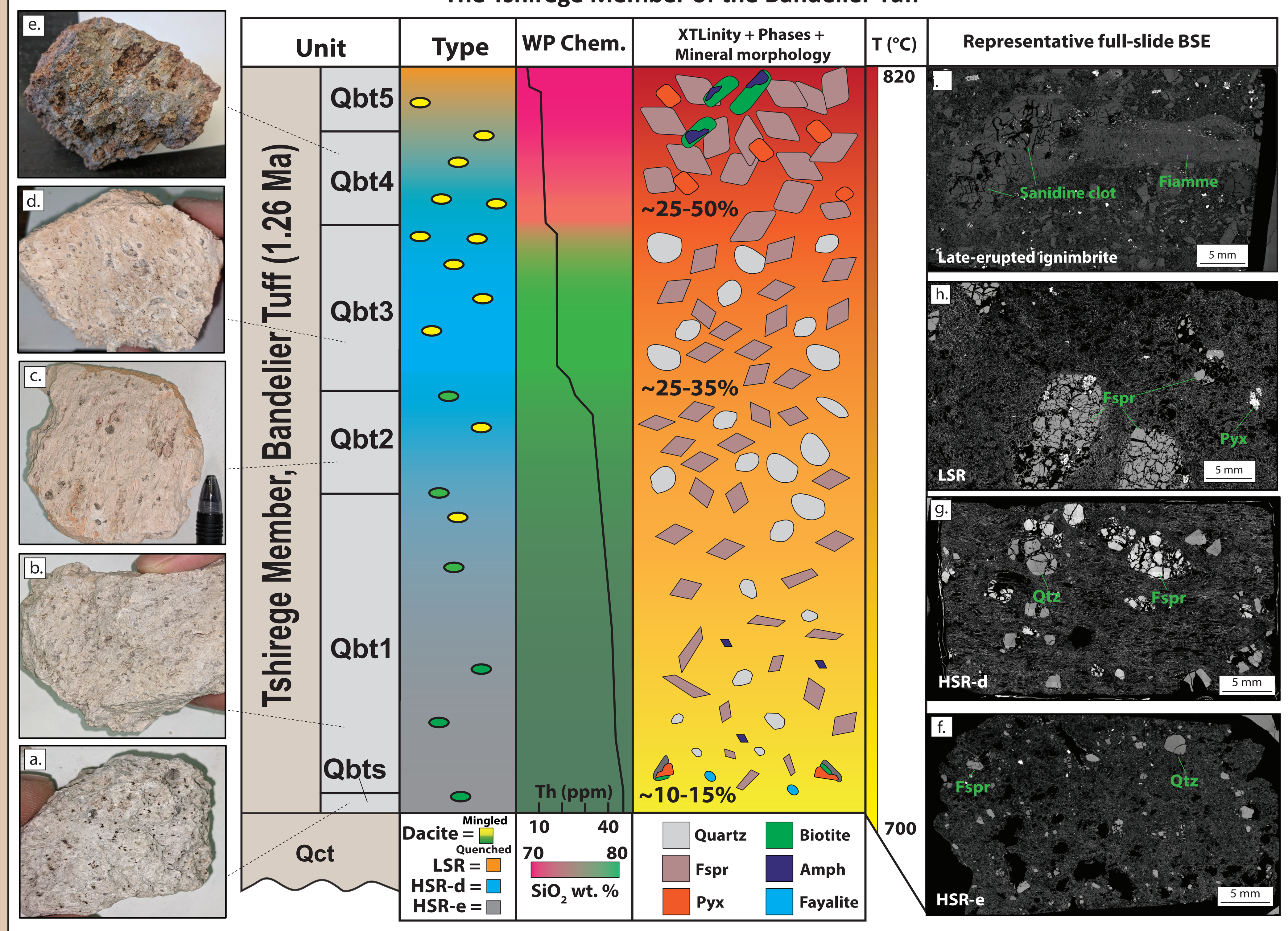

Fig 2. Detailed stratigraphic section summarizing data from this study (n = 142 whole-pumice samples). **a.-e.** are representative hand samples from the Plinian up section to late-erupted crystal-clot pumices in Qbt4. Note the increase in crystallinity and crystal morphology from euhedral (early erupted) and thermally rounded (late erupted). **f.-i.** are accompanying full-slide back-scatter electron maps of pumices from the different chemical groups represented in Fig. 3 & 4. See Fig. 3a for correlation of Qbt# vs chemical pumice type. Stratigraphic column with Q units is modified from Goff et al. (2014) using unit names from Warren et al. (2007).

5. Thermal Constraints

Aware of the uncertainties involved in mineral thermobarometry (typically worse then ±30 °C and ±200 MPa), we present and tabulate the results from this study along with previous authors in Tables 1 and 2.

Opx-Liquid:

We use the orthopyroxene-liquid equilibrium thermobarometer from Putirka (2008, eq. 28a); after filtering for equilibrium, 11 LSR pyroxene and 109 combined glass analyses yield 197 equilibrium pairs. Applying kernel distribution analyses, these data suggest three statistically meaningful temperatures of 785.5, 801, and 809 °C (within calibration error) with an average of 807 ± 7 °C and one statistically meaningful pressure of 0.16 GPa with an average of 0.148 ± 0.04 GPa (Fig. 11).

Ti-in-quartz:

Multiple calibrations of the Ti-in-quartz thermometer on quartz-glass pairs from the HSR-d magma (Boro et al., 2021) give temperatures between 748-786 °C for a constant a(TiO2) for the system, assuming buffering of Ti by oxides and 727-762 °C if it is calculated by changing the a(TiO2) based on the compositions of the glasses.

Feldspar-liquid thermometer:

The feldspar liquid thermometer of Putirka (2008) was applied to 71 feldspars with matching equilibrium pairs and yields a statistical meaningful average of 714 °C ± 1.7 °C for the HSR-e (Fig #). Applications to the other pumice types yielded ~783 °C for the HSR-d, and ~785 °C for the LSR. However fewer sample pairs passed the equilibrium test, suggesting thermal effects of recharge magmas are limiting the usefulness of this thermometer for these two pumice types. Water concentrations in melt inclusions throughout the unit are measured to be ~2-5 wt. % (Waelkens et al. (2021).

Our temperature data indicate that at the time of eruption, there was ~95 ±30 °C stratification in the Tshirege Magma chamber.

Liq-Fspr Thermometry

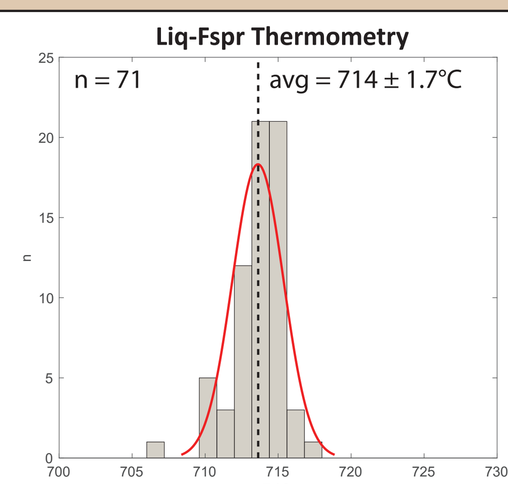

Opx-liquid thermometer

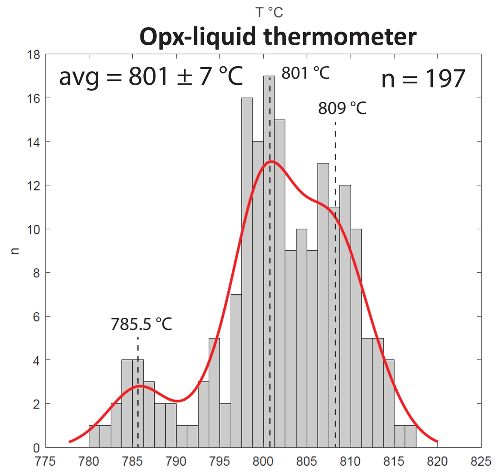

Table 1

Temperatures °C (This study)

	Two-pyroxene	Amphibole-liquid	Feldspar-liquid	Ti-in Quartz (Boro et al. (2021)) α TiO2	Ti-in Quartz (Boro et al. (2021)) γ TiO2
Qbt4	810-840	-	-	-	-
LSR	790-824	-	785	-	-
HSR-d	-	-	783	748-786	727-762
HSR-e	-	725	736	-	-

Table 2

Temperatures °C (previous studies)

Units (Warren et al., 2007)	Fe-Ti oxide	Temperatures (Warshaw and Smith) Magnetite-Fayalite	Two-pyroxene-liquid Clino-	Two-pyroxene-liquid Ortho-
Qbt-5	837	-	840	770
Qbt-4	-	-	-	-
Qbt-3	-	-	-	-
Qbt-3	-	-	760-786	800-810
Qbt-2	-	746-753	700	800
Qbt-1	-	706-726	-	-
Tsankawi	697	-	-	-

6. Thermal modeling

We use Energy2D heat-flow simulations to better understand the temperature stratification of the Tshirege magma chamber. In this case, the thermal properties of the country rock are set to that of granite with a thermal gradient of 25 °C/km and the magma chamber is treated as rhyolite liquid in two scenarios: (1) a magma chamber with a pre-existing thermal stratification and (2) a magma chamber with a homogenous temperature. The recharge block is treated as dacite liquid. The recharge event is modeled as instantaneous. Although there is evidence that it likely happened incrementally over the course of thousands of years, the heat loss out of the system to country rock in that time is minimal.

The dacite is interpreted to have been ~850-900 °C at the time of emplacement (Boro et al. 2020), and we use a starting temperature of 1000 °C to counteract any latent heat of crystallization effects. Additionally, the amount of heating in the rhyolite should be considered a maximum as no heat from melting is taken into account. This model assumes convection does not occur due to the lack of magmatic overturn recorded in the whole pumice samples.

These models show that a recharging body with 1/10th the volume of the rhyolite only carries enough thermal energy to raise the temperature of a stratified chamber up to ~600 m above the intrusion, and heating above that is minimal. We attempted a variety of recharge body shapes and orientations, and found this setup gave us the maximum amount of heating. The unstratified chamber does not get enough heating to loosen the thermal gradient recorded, suggesting there was likely already a thermal gradient prior to recharge.

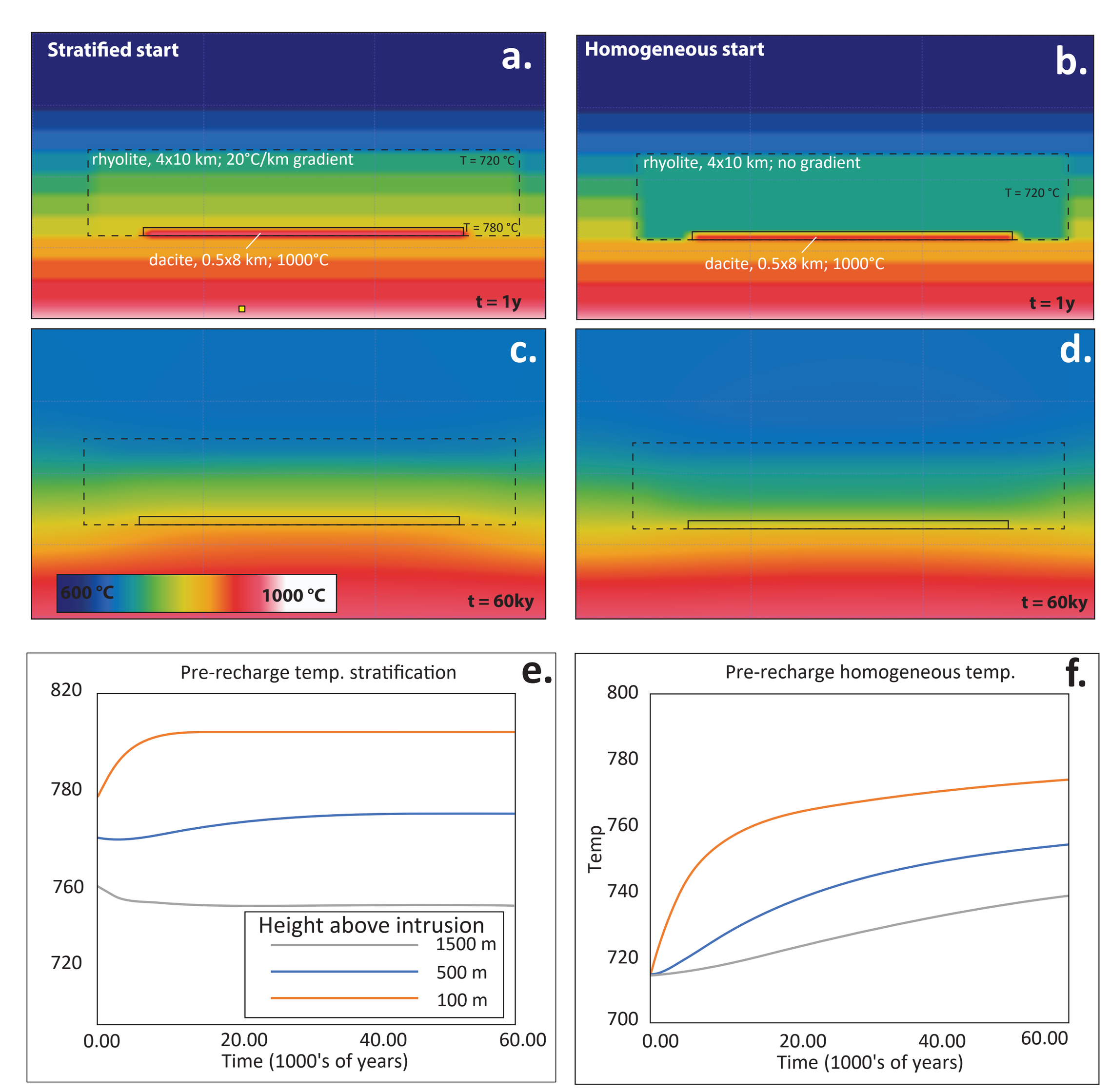

Fig. 5 a-d. Thermal models at 1 y (**a.** and **c.**) and 60ky (**b.** and **d.**) starting with a thermally stratified chamber (**a.**) and a thermally homogeneous chamber (**b.**). The dashed line represents the outline of the rhyolite body, and the thin black line represents the outline of the intrusion. **e. & f.** track the temperature change at various heights above the intrusions for the two scenarios.

3. Whole-pumice v. ignimbrite chemistry

Figure 3 shows trace element plots for Tshirege whole-pumice analyses as well as bulk ignimbrite samples from Brunstad (2002) and Goff et al. (2014). These graphs lead us to the interpretation that whole-pumice samples represent three distinct magmas which mixed or during the eruption or post-emplacement welding to produce the trends present in the whole-ignimbrite samples from previous studies. Whole-pumice samples from the HSR-d, LSR, and dacite magmas plot within multi-endmember mixing space, suggesting at least some pre-eruptive mixing or convective stirring in the lower portions of the Tshirege magma chamber, which was stopped by eruption before complete homogenization. Some feldspars from the LSR contain An65 cores, suggesting mixing and incorporation of recharging magma.

The enrichment in Si in HSR-d past the granite minimum value of 77.8 wt. %, and negative correlation of Nb with increasing Zr in the HSR-d and LSR magmas, are impossible to explain by a simple model of fractional crystallization combined with mixing of recharge magmas. Boro et al. (2021) present melt inclusion chemical data which suggests that much of the Tshirege magma is the result of partially melting a cumulate pile of quartz and sanidine with minor phases present.

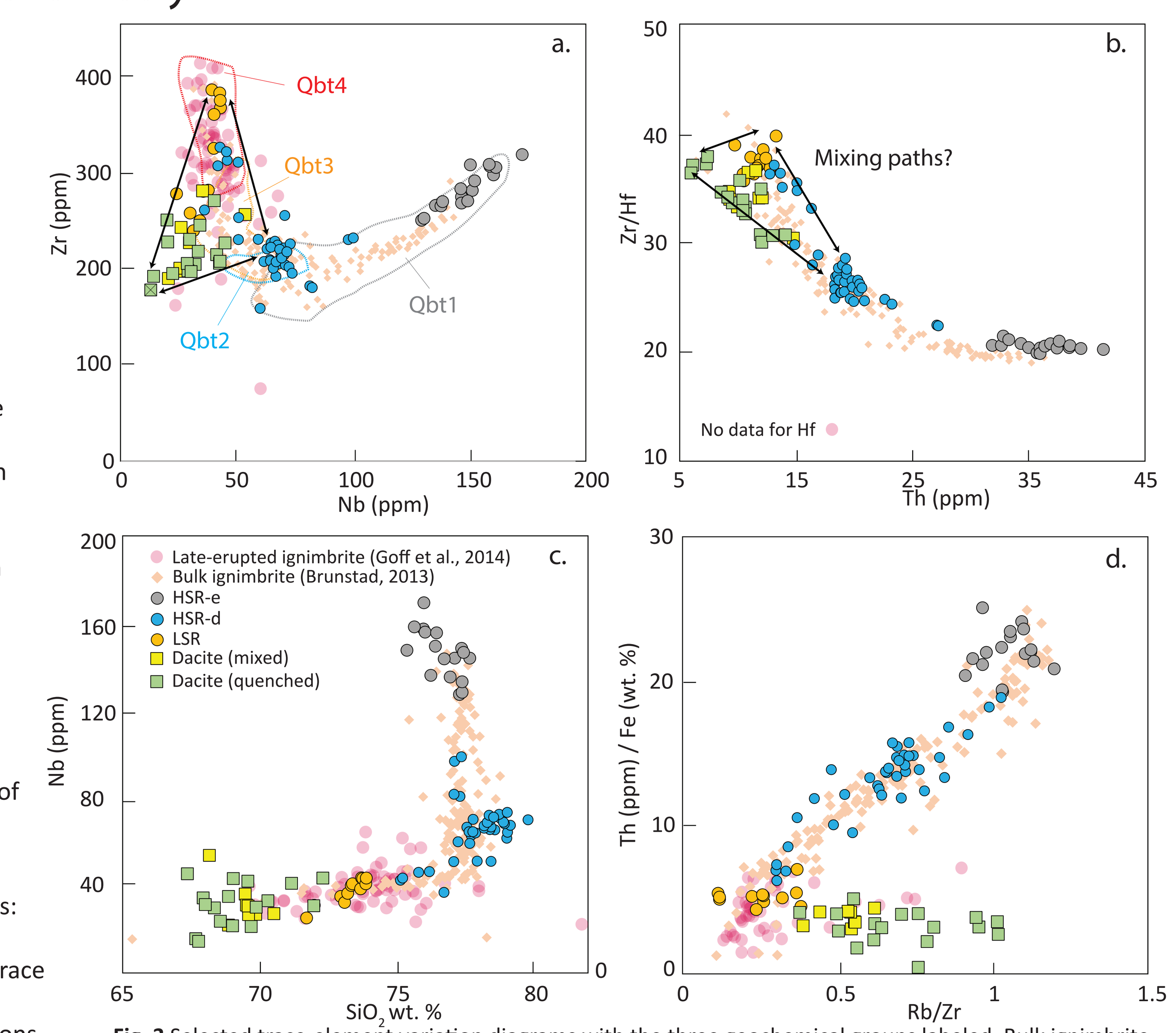

Fig. 3 Selected trace-element variation diagrams with the three geochemical groups labeled. Bulk ignimbrite data and Qbt1-4 regions in **a.** are from Brunstad (2002). Qbt4 bulk ignimbrite data from Goff et al. (2014)

4. Melt inclusion chemistry

Melt inclusions in Tshirege quartz come in two main forms: faceted, located in crystal cores and unfaceted, located in crystal rims (Boro et al., 2021). Depletion of compatible trace elements in crystal core inclusions (e.g. Ba), and more abundant compatible trace elements in crystal rim inclusions leads to the interpretation that faceted inclusions in crystal cores formed early, prior to melting, and the unfaceted melt inclusions in crystal rims were captured late, after melting of cumulates.

Figure 4 shows Ti/Th and La/Th plotted vs Rb/Ba for adhered glass, faceted, and unfaceted melt inclusions. Faceted LSR inclusions were used as a starting point for modeling the evolving liquid during fractionation because they are the probably the earliest fractioned. This predicts ~50% crystallization to produce the most evolved faceted MI. On this plot, there are three distinct groupings. This can be explained by the following scenario:

1. The pre-fractional crystallization original melt is recorded in faceted LSR inclusions.
2. Faceted inclusions located in the center of crystals in the HSR-e and HSR-d record this melt as it evolves following the FC model.
3. The evolved melt mixes to varying degrees with melted ~5% alkali feldspar and 5% quartz which enriches that liquid in feldspar components (Ba and Sr), thus drastically decreasing Rb/Ba, and unfaceted melt inclusions in HSR-e quartz capture that liquid. Ti/Th and La/Th ratios are not affected due to low percent mixes of only melted feldspar and quartz.
4. Melting of more of the mush, including trace phases, forces the melt along a negative slope away from the evolved fluid for both Ti/Th and La/Th. This does not mix with HSR-e melt.

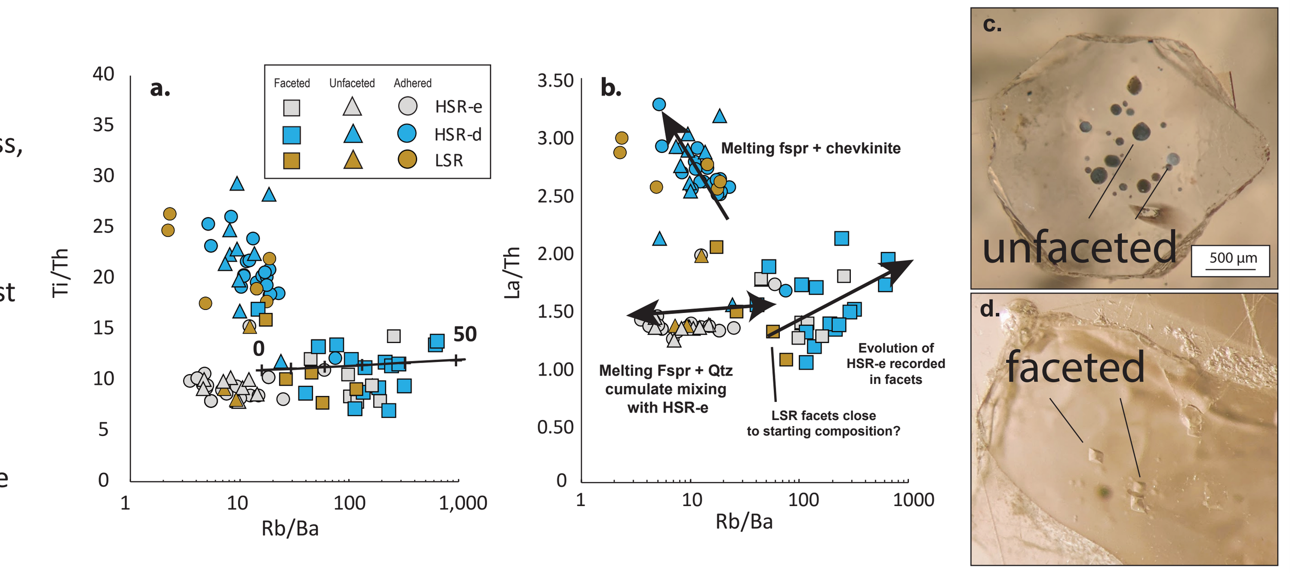

Fig. 4 Two bivariate plots with a.Rb/Ba vs Ti/Th and b. Rb/Ba vs La/Th. Note similar trends in both graphs and log scale for x-axes. Fractional crystalization model labled on **a.** for 50% fractionation trend. Faceted LSR inclusions are used as the starting condition for FC modeling. LSR and HSR-d melt and unfaceted inclusions record melting of feldspar + chevkinite in the crystal mush.

7. MELTS Modeling

For list of references, please email author

Rhyolite-MELTS was used to model the behavior of total crystallinity for average LSR samples. (Figure 12). For purposes of illustration, we assume a relatively dry crystal mush of ~1.5 wt. % total H2O, stored at 0.2 GPa (two-pyx and amphibole-liquid barometry) which places the mush at ~68% crystallinity. Adding 1 wt. % water from addition of water from a recharge magma undergoing second boiling plus heating by ~10-20 °C completely resorbs quartz, and results in a modal percent reduction of phenocrysts to~30%, which agrees with LSR petrographic observations.

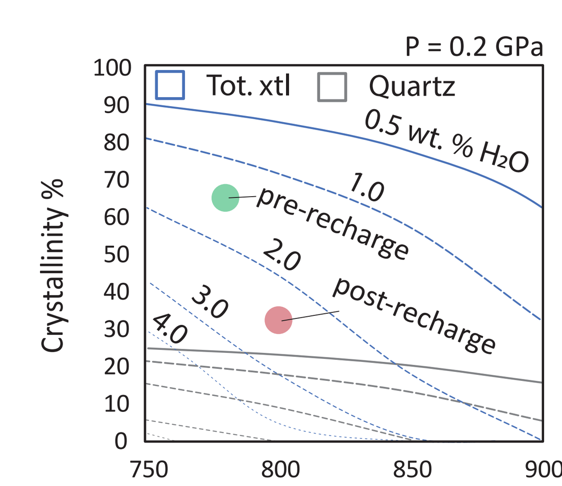

Fig. 6 Rhyolite-MELTS modeling for LSR magma.

8. Conclusions

1) There was a pre-eruptive temperature stratification of ~95 °C of the Tshirege magma chamber.
2) The earliest erupted material was unaffected by thermal or volatile influences from recharging magma.
3) Whole-pumice vs. whole ignimbrite chemical data show most of the erupted material did not experience mixing or overturn prior to the eruption, suggestion convection was shut off and did not restart prior to the eruption even after recharge.
4) Thermal modeling shows that there was likely a pre-recharge thermal stratification and heating alone cannot loosen a crystal mush from critical crystality (~65-70%) to observed erupted crystality (~25-35%).
5) Rhyolite-MELTS modeling shows that addition of water from second boiling of recharge magmas can assist in mush melting along with heating.